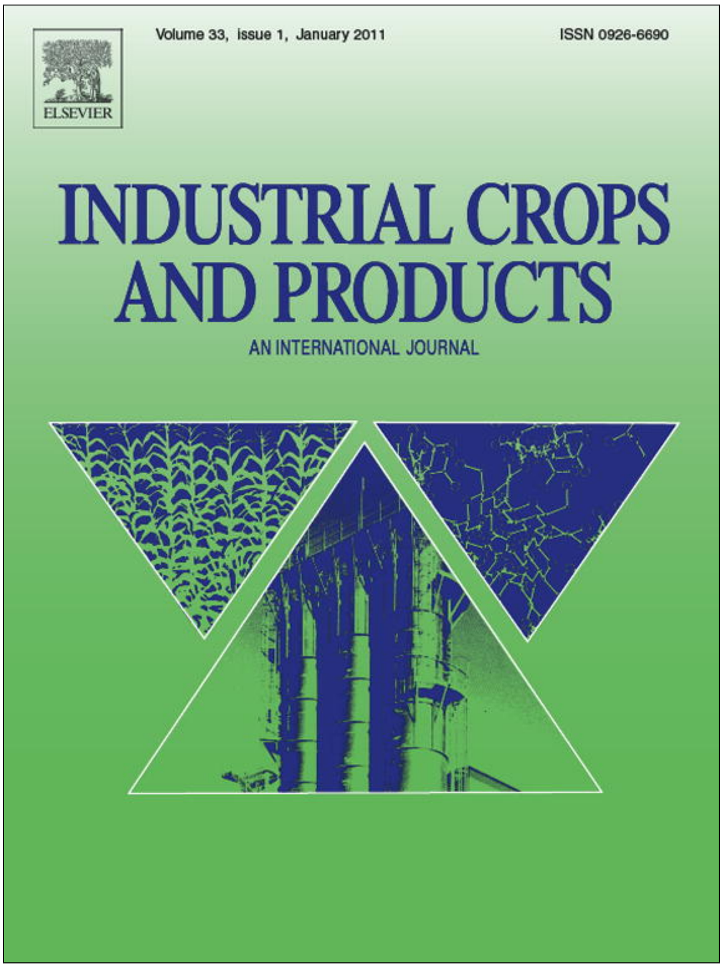
Volume 33, issue 1, January 2011
ISSN 0926-6690
ELSEVIER
INDUSTRIAL CROPS AND PRODUCTS
AN INTERNATIONAL JOURNAL

Industrial Crops and Products 37 (2012) 178–185

Contents lists available at SciVerse ScienceDirect

Industrial Crops and Products

journal homepage: www.elsevier.com/locate/indcrop

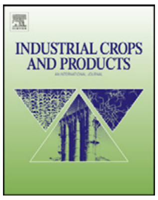

Preparation of peanut hull-based activated carbon by microwave-induced phosphoric acid activation and its application in Remazol Brilliant Blue R adsorption

Zhuo-Ya Zhong[a,c], Qi Yang[a,c,*], Xiao-Ming Li[a,b,c,*], Kun Luo[a,c], Yang Liu[a,d], Guang-Ming Zeng[a,c]

[a] College of Environmental Science and Engineering, Hunan University, Changsha 410082, PR China
[b] College of Environment, Guangxi University, Nanning 530004, PR China
[c] Key Laboratory of Environmental Biology and Pollution Control (Hunan University), Ministry of Education, Changsha 410082, PR China
[d] Hunan Engineering Research Center of Urban and Rural Domestic Waste Treatment and Disposal, Changsha 410008, PR China

ARTICLE INFO

Article history:
Received 12 September 2011
Received in revised form 2 December 2011
Accepted 14 December 2011

Keywords:
Activated carbon
Microwave
Peanut hull
Remazol Brilliant Blue R
Response surface methodology

ABSTRACT

Peanut hull, an agricultural solid waste abundantly available in China, was utilized as a precursor for preparation of activated carbon via microwave induced phosphoric acid chemical activation. To optimize the preparation conditions, the effects of the concentration of phosphoric acid, microwave power and radiation time on the adsorption property (expressed in terms of the iodine number) and yield of the activated carbon were investigated by response surface methodology (RSM). The optimum activated carbon obtained with phosphoric acid concentration of 33.04 vol.%, microwave power of 500.70 W and radiation time of 9.8 min had a iodine number of 813.11 mg/g and yield of carbon of 42.12%. The prepared activated carbons were characterized for their surface chemistry by FTIR, as well as for their porous and morphological structure by SEM and nitrogen adsorption at 77.3 K. The adsorption behavior was well described by the Langmuir isotherm model, showing a monolayer adsorption capacity for Remazol Brilliant Blue R (RBBR) of 149.25 mg/g. The investigation of adsorption kinetics indicated that the process closely follow the model of intraparticle diffusion, a pseudo-second-order chemisorption model.

1. Introduction

Activated carbon, with strong adsorption capacity due to its high specific surface area, adequate pore size distribution and relatively high mechanical strength, has been widely employed in air pollution control, food processing as well as wastewater treatment (Guo et al., 2007; Mudoga et al., 2008; Crini, 2006). A wide range of raw lignocellulosic materials such as coal, peat, wood and various agricultural by-product, have been utilized for the preparation of activated carbon. Peanut is a widely planted leguminous crop in China and the output is estimated to be approximately around 14.71 million tons in 2008. With an estimate of 30% waste biomass generation, the projected peanut hulls could reach 4.4 million tons (Li et al., 2010), most of which were discarded as solid waste or burned off in stacks causing the resource dissipation and environmental pollution. As the peanut hull is rich of cellulose, hemicellulose and polymer materials, it has the potential to be a good precursor for the production of activated carbon.

Generally, the physical and chemical activation methods are employed in preparation of activated carbon to enhance their adsorption capacity. In chemical activation, the raw material is firstly impregnated by activating agents such as H_3PO_4, KOH, or K_2CO_3 (Zuo et al., 2009; Basta et al., 2009; Li et al., 2008) before thermal activation, and a higher yield and better developed pore structure of activated carbon could be obtained compared with physical activation. Heating, as an essential step for chemical activation, is conventionally operated in a furnace which resulting in a surface heating and leading to adverse effect on the product quality since the non-uniform temperature for different shapes and sizes of materials. However, microwave-induced chemical reaction can avoid this problem because the conversion of microwave energy is not by conduction or convection as in conventional heating, but by dipole rotation and ionic conduction inside the particles (Yuen and Hameed, 2009). Therefore, the tremendous thermal gradient from the interior of the char particle to its cool surface allows the microwave-induced reaction to proceed more quickly and effectively at lower temperature, resulting in energy savings and time shortening.

RSM has been applied widely in the process optimization (Mahalik et al., 2010; Abnisa et al., 2011), and it was found to

---

* Corresponding authors at: College of Environmental Science and Engineering, Hunan University, Changsha 410082, PR China. Tel.: +86 731 88823967; fax: +86 731 88822829.
E-mail addresses: yangqi@hnu.edu.cn (Q. Yang), xmli@hnu.edu.cn (X.-M. Li).

0926-6690/$ – see front matter © 2011 Elsevier B.V. All rights reserved.
doi:10.1016/j.indcrop.2011.12.015

be a useful tool to study the interactions of two or more factors (Karacan et al., 2007). The microwave-induced chemical activation as a novel method for the preparation of activated carbon can not only save energy and shorten time of preparation, but also enhance the formation of activated carbon with higher surface area and well-developed porosity. Currently no study has been reported on the preparation of activated carbon from peanut hull via microwave activation and the conditions optimization using the RSM approach. Here, we investigated the effects of concentration of phosphoric acid, microwave power and radiation time on the carbon adsorption property (expressed in terms of the iodine number) and yield of carbon by RSM. The low-cost peanut hull-based activated carbon was fully characterized and subsequently used as an adsorbent for RBBR removal. Moreover, the adsorption equilibrium and kinetic of RBBR was outlined and discussed.

2. Materials and methods

2.1. Preparation of activated carbon

The peanut hull obtained from agricultural suburb of Changsha, Hunan Province of China, was washed with deionized water to remove dust, dried at 80 °C to get rid of the moisture and other volatile impurities, crushed and sieved into a uniform size of less than 2.0 mm. The proximate analysis of the peanut hull represented in weight percent was as follows: moisture 10.85%, cellulose 16.91%, hemicellulose 10.11%, lignin 27.43% and ash 2.62%.

The powdered peanut hulls with the mass of 3 g were firstly impregnated with 10 mL of different concentration of phosphoric acid (6.48–48.52 vol.%) for 24 h. The impregnated precursor was activated in a sequence MW heating apparatus (LWMC-205, Nanjing Robiot Co., Ltd, China) under nitrogen flow of 40 mL/min. Then the product was washed sequentially with 0.5 M HCl, hot water and cold distilled water until the pH of washing effluent reached 6.0–7.0. The final product was dried at 105 °C to a constant weight and sieved into uniform granules for further use.

2.2. Experimental design and statistical analysis

RSM is a statistical technique for modeling and analysis of problems in which a response of interest is influenced by several factors (Duan et al., 2011). In this paper, a standard RSM design, known as central composite design (CCD) was applied to study the variables for preparing the activated carbons from peanut hull via microwave-induced activation. The dependant variables selected were the concentration of phosphoric acid by volume (x_1), microwave power (x_2) and radiation time (x_3). A full factorial CCD for the three variables, consisting of 8 factorial points, 6 axial points and 6 replicates at the center points, were employed and a total of 20 experiments were obtained from Eq. (1) (Azargohar and Dalai, 2005):

$$N = 2^n + 2n + n_c = 2^3 + 2 \times 3 + 6 = 20 \tag{1}$$

where N is the total number of experiments and n is the number of factors.

The response variable (Y) that represented iodine number (Y_1) or yield (Y_2) was fitted by a second-order quardratic polynomial equation:

$$Y = \beta_0 + \sum_{i=1}^{3} \beta_i x_i + \sum_{i=1}^{3} \beta_{ii} x_i^2 + \sum_{i=1}^{3} \sum_{j=i+1}^{3} \beta_{ij} x_i x_j \tag{2}$$

where Y is the response variable, x_i and x_j are the coded variables which determine Y, β_0 is the constant coefficient, β_i is the linear coefficients, β_{ij} is the interaction coefficients, β_{ii} is the quadratic coefficients.

The experimental data were analyzed using statistical software design expert software version 7.1.5 (STAT-EASE Inc., Minneapolis, USA) for regression analysis and to evaluate the statistical significance of the equation.

2.3. Characterization of activated carbon

The adsorptive property of activated carbon was determined by iodine adsorption capacity which indicated milligrams of iodine adsorbed by a gram of activated carbon (mg/g), according to the Standard Testing Methods of PR China (GB/T12496.8-1999). The yield was defined as grams of activated carbon per gram peanut hull utilized for activation.

The surface morphology of the peanut hull before and after activation was examined using scanning electron microscopy (SEM) (JSM-6400F, Japan Electron Optics Laboratory Ltd. Corp., Japan).

The surface physical properties of the activated carbons were characterized with an automatic chemisorption & physisorption analyzer (Quantachrome Instrument Corp., USA), using N_2 as the adsorbate at 77.3 K. The surface area (S_{BET}) was calculated by the BET equation, and the pore volume (V_T) was obtained from the adsorption isotherm at $P/P_0 = 0.95$.

The surface functional groups of samples were determined by Fourier transform infrared (FTIR) spectroscopy (Nicolet 6700, Nicolet Instrument Corp., USA) with the scanning range of 4000–400 cm^{-1}.

2.4. Equilibrium adsorption studies

Remazol Brilliant Blue R (RBBR) purchased from Sigma–Aldrich Company Ltd., an anthraquinone-based dye, was chosen as the adsorbate in this study. Deionized water was used to prepare all solutions. The chemical formula of RBBR is $C_{22}H_{16}N_2Na_2O_{11}S_3$, with the molecular weight of 625.56 g/mol.

Equilibrium adsorption studies were conducted in a set of 50 mL glass-stoppered flasks containing 0.04 g activated carbon and 25 mL various initial concentration of RBBR solution (25–300 mg/L). The flasks were agitated in a mechanical shaker at 170 rpm and 20 °C until the equilibrium was reached. The concentration of RBBR was determined using UV–visible spectrophotometer (UV-754N Shanghai, China) at maximum wavelength of 591 nm. The RBBR uptake at equilibrium, q_e (mg/g), was calculated by Eq. (3):

$$q_e = \frac{(C_0 - C_e) \times V}{W} \tag{3}$$

where C_0 and C_e (mg/L) are the liquid-phase concentration of RBBR at initial and at equilibrium, respectively. V (L) is the volume of the solution and W (g) is the mass of dry activated carbon.

3. Results and discussion

3.1. Preparation of activated carbons

3.1.1. Development of regression model equation

CCD was used to develop correlation between the activated carbon preparation variables to the iodine number and yield. Table 1 shows the complete design matrixes together with both the response values obtained from the practical experiment. Runs 15–20 at the center point were used to check the experimental error. The iodine number was found to range from 437.07 to 1002.83 mg/g, while the yield of carbon obtained ranged from 17.41 to 47.51%. In light of the sequential model sum of squares, the models were chosen based on the highest order polynomials where the additional terms were significant and the models were not aliased. For both responses of iodine number and yield, the quadratic models were selected, as suggested by the software. The final empirical

Table 1
Experimental design matrix and results.

Run	Levels			Activated carbon preparation variables			Iodine number	Yield
				X_1 (vol.%)	X_2 (W)	X_3 (min)	Y_1 (mg/g)	Y_2 (%)
1	−1	−1	−1	15.00	400.00	6.00	437.07	46.97
2	+1	−1	−1	40.00	400.00	6.00	619.52	47.51
3	−1	+1	−1	15.00	600.00	6.00	652.06	30.29
4	+1	+1	−1	40.00	600.00	6.00	667.43	38.91
5	−1	−1	+1	15.00	400.00	12.00	533.87	36.70
6	+1	−1	+1	40.00	400.00	12.00	683.40	36.88
7	−1	+1	+1	15.00	600.00	12.00	655.25	30.21
8	+1	+1	+1	40.00	600.00	12.00	1002.83	17.41
9	−1.682	0	0	6.48	331.82	9.00	466.79	32.60
10	+1.682	0	0	48.52	668.18	9.00	620.11	42.75
11	0	−1.682	0	27.50	500.00	9.00	674.42	42.74
12	0	+1.682	0	27.50	500.00	9.00	632.89	30.78
13	0	0	−1.682	27.50	500.00	3.95	754.27	47.36
14	0	0	+1.682	27.50	500.00	14.05	866.07	26.57
15	0	0	0	27.50	500.00	9.00	754.27	40.72
16	0	0	0	27.50	500.00	9.00	754.31	42.27
17	0	0	0	27.50	500.00	9.00	748.13	41.32
18	0	0	0	27.50	500.00	9.00	754.08	41.46
19	0	0	0	27.50	500.00	9.00	755.43	40.52
20	0	0	0	27.50	500.00	9.00	748.87	40.98

models in terms of coded factors for the iodine number (Y_1) and yield (Y_2) were shown in Eqs. (4) and (5), respectively.

$$\begin{aligned} Y_1 = {} & 754.59 + 69.77x_1 + 46.41x_2 + 50.33x_3 + 3.87x_1x_2 \\ & + 37.41x_1x_3 + 22.24x_2x_3 - 76.15x_1^2 - 37.18x_2^2 + 18.16x_3^2 \end{aligned} \quad (4)$$

$$\begin{aligned} Y_2 = {} & 41.92 + 1.00x_1 - 5.22x_2 - 5.67x_3 - 0.61x_1x_2 - 2.72x_1x_3 \\ & - 0.085x_2x_3 - 1.75x_1^2 - 2.07x_2^2 - 2.00x_3^2 \end{aligned} \quad (5)$$

Positive sign in front of the terms indicates synergistic effect, whereas negative sign indicates antagonistic effect. The quality of the model developed was evaluated based on the correlation coefficients (R^2), which were 0.812 for Eq. (4) and 0.887 for Eq. (5). Both the R^2 values of iodine adsorption and carbon yield were relatively high, indicating a good agreement between the experimental data and the model prediction.

The adequacy of the models was further justified through the analysis of variance (ANOVA). The ANOVA for the quadratic model for iodine adsorption is listed in Table 2. From the ANOVA for response surface quadratic model for iodine number, the model F-value of 4.81 for iodine number implied that the model was significant. Values of Prob. > F less than 0.05 indicated that the model terms were significant. In this case, x_1, x_2, x_3, x_1^2 were significant to the response of iodine number, and $x_1x_2, x_1x_3, x_2x_3, x_2^2, x_3^2$ were all insignificant model terms. From the ANOVA for activated carbon yield is shown in Table 3, the model F-value of 8.75 and Prob. > F of 0.0011 revealed that the model was significant as well. In this case, x_2, x_3 were significant model terms whereas $x_1, x_1x_2, x_1x_3, x_2x_3, x_1^2, x_2^2, x_3^2$ were all insignificant to the response.

3.1.2. Iodine adsorption

The most important characteristic of activated carbon was its adsorption capacity, which was strongly influenced by the preparation conditions. Based on the F-value shown in Table 2, all the three parameters chosen in this study were found to have significant effects on the iodine adsorption of peanut hull-based activated carbon, whereas the concentration of phosphoric acid (x_1) showed the greatest significant effect on this response, with the highest F value of 11.33, while microwave power and activation time showed slight effects on the response for iodine adsorption.

Fig. 1(a) shows the three-dimensional response surface which is constructed to show the interaction effects of concentration of phosphoric acid and microwave power on iodine number. For this plot, the radiation time was fixed at zero level (t = 9 min). As seen from Fig. 1(a), the iodine number rapidly increased with the increase of phosphoric acid concentration and microwave power firstly, with the maximum iodine number of about 786 mg/g, and then gradually decreased with further increase of the two variables. It might attribute that phosphoric acid occupied a volume which hindered the shrinkage, thus leading to the formation of porosity when it was extracted by washing (Girgis et al., 2002), however, excessive phosphoric acid could not further promote the porosity since an insulating layer might be formed (Molina-Sabio and Rodriguez-Reinoso, 2004). Meanwhile, higher activation temperature induced by higher microwave power led to a reduction in the activation energy for the carbon–acid reaction and more active sites and pores were formed. Moreover, when activation temperature reached a certain value, the activated carbon exhibited lower surface area and lacked well developed pores, as well as the high percentage of mesopores and macropores (Arami-Niya et al., in press; Lua and Guo, 2000), probably because the pores of activated carbon would be widen or burnt off under more intense microwave radiation.

Fig. 1(b) illustrates the three-dimensional response surfaces of the combined effect of phosphoric acid concentration and radiation time on the iodine number, at a microwave power of 500 W. The iodine number was found to increase gradually with the radiation time increased from 6 to 12 min. The longer microwave radiation time led to more active sites and more pores formed inside the samples, which could enhance the adsorption capacity. However, Li et al. (2008) indicated that it was not necessary to prolong activation time beyond a certain value, because the pores of carbons would be burnt off by microwave heating which may lower the adsorption capacity.

3.1.3. Activated carbon yield

Referring to Table 3, both the microwave power (x_2) and activation time (x_3) were found to have significant effects on the activated carbon yield, with activation time imposing the greatest effect on it. However, the interaction effects between the variables were all less significant.

Fig. 2 represents the effects of microwave power and radiation time on the yield of activated carbon with the phosphoric acid

Table 2
ANOVA for response surface quadratic model for iodine number.

Source	Sum of squares	Degree of freedom	Mean square	*F* value	Prob. > *F*
Model	253,916.4	9	28,212.94	4.81	0.0110
x_1	66,474.1	1	66,474.1	11.33	0.0072
x_2	29,420.72	1	29,420.72	5.02	0.0490
x_3	34,589.35	1	34,589.35	5.90	0.0356
x_1x_2	119.93	1	119.93	0.020	0.8891
x_1x_3	11,197.22	1	11,197.22	1.91	0.1972
x_2x_3	3956.60	1	3956.60	0.67	0.4306
x_1^2	83,557.94	1	83,557.94	14.24	0.0036
x_2^2	19,924.02	1	19,924.02	3.40	0.0951
x_3^2	4750.61	1	4750.61	0.81	0.3893
Residual	58,661.43	10	5866.14	–	–

Table 3
ANOVA for response surface quadratic model for yield.

Source	Sum of squares	Degree of freedom	Mean square	*F* value	Prob. > *F*
Model	1024.32	9	113.81	8.75	0.0011
x_1	13.55	1	13.55	1.04	0.33
x_2	372.81	1	372.81	28.66	0.0003
x_3	439.17	1	439.16	33.76	0.0002
x_1x_2	3.00	1	3.00	0.23	0.64
x_1x_3	59.30	1	59.30	4.56	0.058
x_2x_3	0.058	1	0.058	0.0044	0.95
x_1^2	43.95	1	43.95	3.38	0.096
x_2^2	61.78	1	61.78	4.75	0.054
x_3^2	57.53	1	57.53	4.42	0.062
Residual	130.10	10	13.01	–	–

concentration fixed at zero level (27.50 vol.%). The activated carbon yield showed a drastically decrease from 45.44% to 32.49% (Fig. 2), due to the continuous loss of weight with the increase of activation time and microwave power. The same trend was found by Deng et al. (2009) and Liu et al. (2010) during the preparation of activated carbon from cotton stalk and bamboo under microwave radiation. Sahu et al. (2010) observed that the yield of activated carbon decreased with increasing carbonization time and carbonization temperature, as more volatiles of samples were released then.

3.1.4. *Process optimization*

The main aim of this study was to find the optimum process parameters in which activated carbon produced should have a high adsorption capacity and a relatively high yield. However, as previously discussed, both these response showed different interest region under the same condition. When Y_1 increases, Y_2 would decrease and vice versa. In order to compromise between these two responses, the function of desirability was applied with Design Expert software version, 7.1.5 (STAT-EASE Inc., Minneapolis, USA). The optimum experimental conditions of prepared activated carbon are given in Table 4, together with the predicted and experimental values of iodine number and activated carbon yield. The optimum operating conditions were calculated as: phosphoric acid concentration of 33.04 vol.%, microwave power of 500.70 W and radiation time of 9.80 min, under which an iodine number of 813.11 mg/g and a activated carbon yield of 42.12% could be reached. The experimental values obtained (Table 4) were in good agreement with the values predicted from the models, with relatively small errors between the predicted and the actual values, which was only 2.83% for iodine number and 5.03% for activated carbon yield.

3.2. *Characterization of activated carbon prepared under optimum conditions*

3.2.1. *Surface morphology analysis*

SEM images of the peanut hull and the activated carbon prepared under optimum conditions are shown in Fig. 3. The surface of raw material (Fig. 3(a)) was fairly smooth without any pores

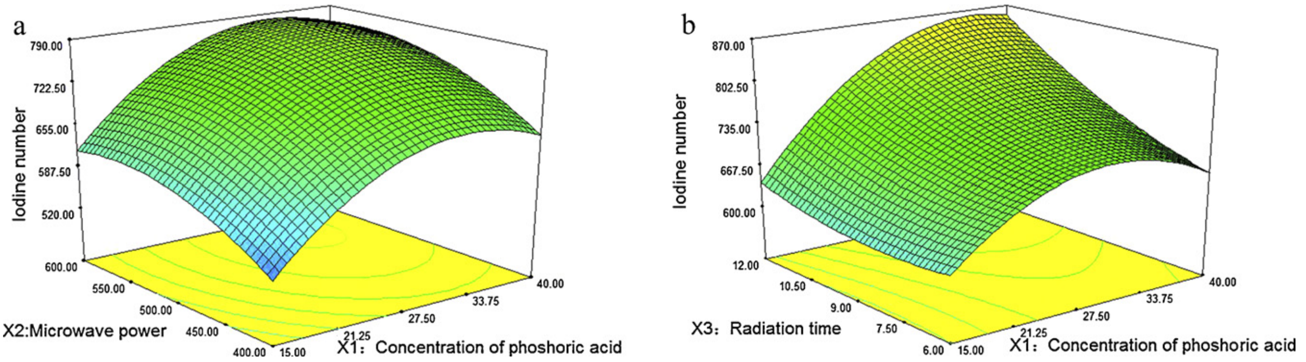

Fig. 1. Three-dimensional response surface plot of iodine uptake: (a) effect of concentration of phosphoric acid and microwave power (radiation time: 9 min); (b) effect of concentration of phosphoric acid and radiation time (microwave power: 500 W).

Table 4
Process optimization validation.

Concentration of H_3PO_4 (vol.%)	Microwave power (W)	Radiation time (min)	Iodine number (mg/g)		Yield (%)	
			Predicted	Experimental	Predicted	Experimental
33.04	500.70	9.80	790.08	813.11	40.00	42.12

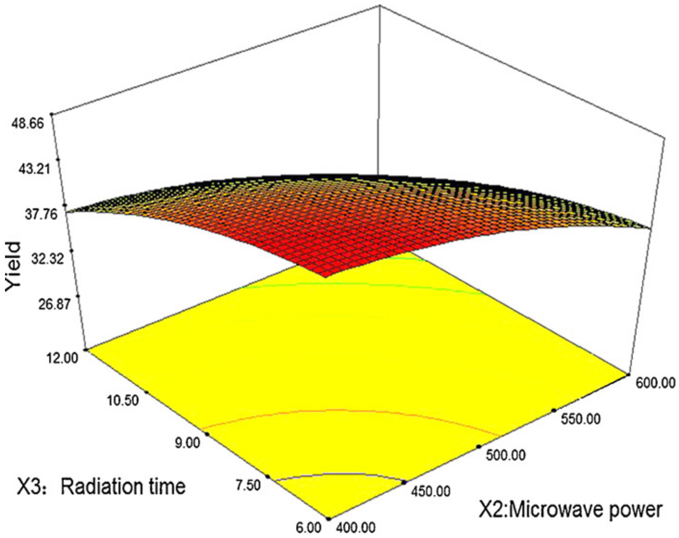

Fig. 2. Three-dimensional response surface plot of activated carbon yield: effect of microwave power and radiation time (concentration of phosphoric acid: 27.50 vol.%).

except for some occasional cracks. After activation the peanut hull transformed into activated carbon with a significant increase in the micro and mesopores. As shown in Fig. 3(b), the external surface of the activated carbon demonstrated a well pronounced and almost uniform pore structure, indicating constitution of new matrix during the activation stage.

3.2.2. *Porous structure analysis*

Nitrogen adsorption is a standard procedure for the determination of porosity of carbonaceous adsorbents. From nitrogen adsorption isotherm analysis, it could be found that the isotherm of peanut hull-based activated carbon presented I–IV character nitrogen isotherm according to the BDDT (Brunauer-Deming-Deming-Teller) classification (Fig. 4), demonstrating that there were microporous with a considerable development of mesopority in the carbon. The pore size distribution for the activated carbon by the Horvath-Kawazoe method shown in Fig. 5 substantiates the amount of pores in the microporous range, with the average pore diameter estimate to be 3.6 nm.

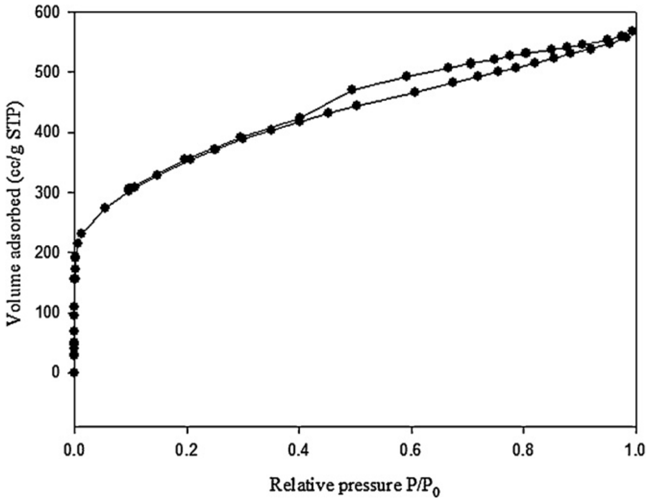

Fig. 4. N_2 adsorption–desorption isotherms at 77.3 K of peanut hull-based activated carbon.

Table 5 summarizes the comparison of the pore structure of microwave irradiated activated carbons from agricultural by-product. The adsorbent prepared in this work showed relatively high S_{BET} of 952.60 m^2/g and V_T of 0.8807 cm^3/g, as compared to some previous works reported in the literatures. This suggested the peanut hull could also form considerable porous structure through microwave-induced chemical activation.

3.2.3. *FTIR analysis*

The FTIR spectra can provide valuable information about the chemical compositions of the materials. The obtained FTIR spectra

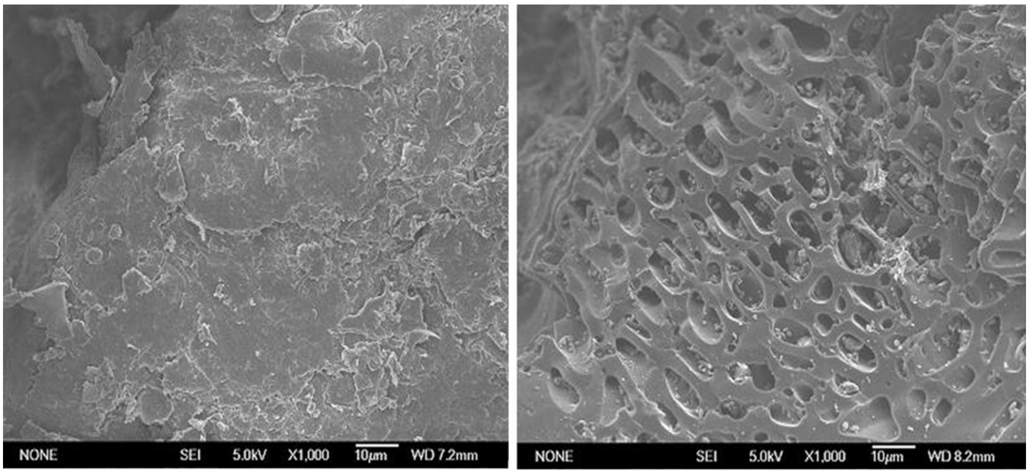

(a) Peanut hulls (b) Activated carbon

Fig. 3. SEM micrographs of the selected samples at 1000× magnification.

Table 5
Comparison of the pore structure of microwave irradiated activated carbons from agricultural by-produce.

Precursors	Activatingagent	S_{BET} (m^2/g)	V_T (cm^3/g)	V_{mic} (cm^3/g)	References
Peanut hull	H_3PO_4	952.60	0.8807	0.2777	This work
Rice husk	KOH	752.00	0.6400	0.2600	Foo and Hameed (2011b)
Cotton stalk	$ZnCl_2$	794.84	0.6300	0.0830	Deng et al. (2009)
Orangepeel	K_2CO_3	1104.45	0.6150	0.2470	Foo and Hameed (2012)
Jatropha hull	–	1350.00	1.0700	0.4366	Duan et al. (2010)
Bamboo	H_3PO_4	1432.00	0.6960	0.5030	Liu et al. (2010)

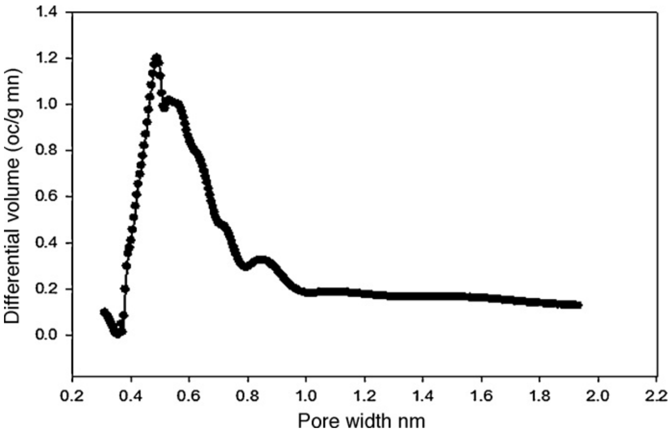

Fig. 5. Pore size distributions of peanut hull-based activated carbon.

(Fig. 6) revealed that the peanut hull contained more bands than the prepared activated carbon, indicating that the surface functional groups of peanut hulls experienced chemical changes during microwave-induce chemical activation. The broad band at about 3646 cm^{-1} for peanut hull was assigned to the O—H stretching vibration of the hydroxyl functional groups including hydrogen bonding (Sahu et al., 2010), but the weakened O—H vibrations was found at about 3444 cm^{-1} for prepared activated carbon owing to the degradation of lignocellulosic and cellulosic material. The intense band at about 2930 cm^{-1} for peanut hull was attributed to the C—H stretching vibration (Aguilar et al., 2003), which disappeared for the activated carbon, indicating that the hydrogen element was removed to a large extent after activation. The bands located at 2362 cm^{-1}, 1570 cm^{-1} and 1215 cm^{-1} in the spectra of the peanut hulls also demonstrated the peanut hull contained large amounts of lignocellulosic material, as lignin was a complex amorphous polymer which was constructed by alkyne group, carbon—carbon bonds and ether link. After microwave-induced chemical activation, the bands located at about 1638 cm^{-1}, attributing to carbonyl —C=O stretching vibration (Lua and Yang, 2004), was present for activated carbon, which possibly owed to the extraction of H element and OH groups from the aromatic rings during the impregnation and heat treatment stages as a result of the dehydration effect of phosphoric acid. The absorption peak around 1120 cm^{-1} indicated the existence of C—O bond in carboxylic or the P=O bond in phosphate esters (Yagmur et al., 2008).

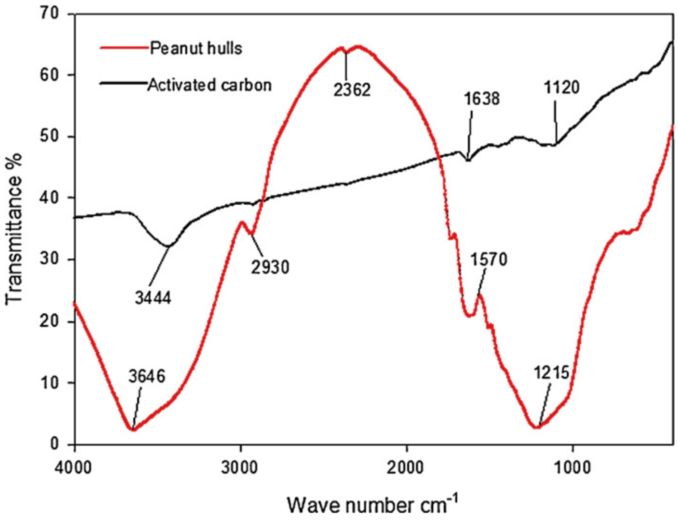

Fig. 6. FTIR spectra of peanut hull and peanut hull-based activated carbon.

3.3. Adsorption of RBBR

3.3.1. Equilibrium adsorption isotherm

The adsorption isotherm indicated how the adsorption molecules distribute between the liquid phase and the solid phase when the adsorption process reached an equilibrium state. In this study, three isothermal models were used for describing the results, namely Langmuir isotherm, Freundlich isotherm, and Temkin isotherm.

The Langmuir isotherm model is valid for monolayer adsorption onto a surface containing a finite number of identical sites of uniform strategies of adsorption with no transmigration of adsorbate in the plane of surface (Weber and Chakkravorti, 1974). It can be represented by the following form:

$$q_e = \frac{K_L q_m C_e}{1 + K_L C_e} \tag{6}$$

where q_e (mg/g) is the equilibrium adsorption capacity, C_e is the equilibrium dye concentration, K_L (L/mg) is the Langmuir constant and q_m (mg/g) is the maximum adsorption capacity.

For Langmuir adsorption isotherm, one of the essential characteristics could be expressed by dimensionless constant called equilibrium parameter, R_L, It can be represented by the following (Hall et al., 1966):

$$R_L = \frac{1}{1 + K_L C_0} \tag{7}$$

where R_L (mg/L) is the Langmuir constant and C_0 (mg/L) is the lowest initial dye concentration. The value of R_L indicated the type of the Langmuir isotherm to be either unfavorable ($R_L > 1$), linear ($R_L = 1$), favorable ($0 < R_L < 1$) or irreversible ($R_L = 0$).

The Freundlich adsorption model is suitable for non-ideal adsorption on heterogeneous surfaces. The empirical model is shown to be consistent with an exponential distribution of active centers, characteristic of heterogeneous surface (Freundlich, 1906), which can be written as below:

$$q_e = K_F C_e^{1/n} \tag{8}$$

where K_F (mg/g) and $1/n$ are the Freundich constants related to the adsorption capacity, adsorption intensity.

The construction of Temkin equation considers the effects of indirect adsorate–adsorbate interactions. Due to the interactions, the heat of adsorption of all the molecules in the layer would

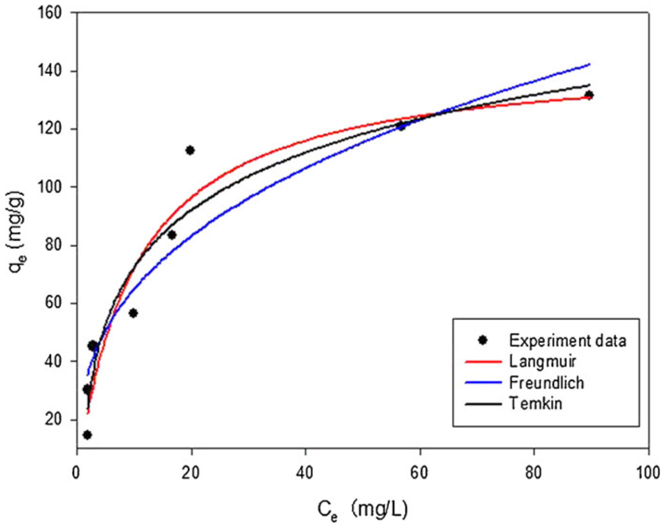

Fig. 7. Comparison of different isothermal models for RBBR adsorption onto peanut hull-based activated carbon.

decrease linearly with coverage (Hall et al., 1966). So, the Temkin isotherm is used in the form as follows:

$$q_e = \left(\frac{RT}{b}\right) \ln(AC_e) \tag{9}$$

where $RT/b = B$, b (J/mol) is the Temkin constant related to heat of sorption, A (L/g) is the Temkin isotherm constant, R is the gas constant (8.31 J/(mol K)) and T (K) is the absolute temperature.

Fig. 7 shows the three fitted model curves and the experimental results of the RBBR adsorption equilibrium isotherm at 20 °C with the peanut hull-based activated carbon prepared under the optimum conditions. The fitting results, i.e. isotherm parameters and the coefficient of determination, R^2, are shown in Table 6. The R^2 of the three models descend in the order of: Langmuir > Temkin > Freundlich. The results revealed that the adsorption of RBBR on activated carbon prepared were described by Langmuir isotherm more than the others, indicating the adsorption of RBBR onto the adsorbent tended to homogeneous and monolayer adsorption. Furthermore, the value of R_L was found to be 0.29, which further confirmed that the Langmuir isotherm was favorable for adsorption of RBBR on the activated carbon. The variation of the adsorption energy b obtained from the Temkin equation was positive, which indicated that the adsorption reaction was exothermic (Hamdaoui, 2006). Similar observations were reported for the adsorption of methylene blue onto the cotton stalks and pistachio nut shells derived microwave irradiated activated carbons (Deng et al., 2010; Foo and Hameed, 2011a).

Table 6
Isotherm constants and regression correlation coefficients for the RBBR adsorption onto peanut hull-based activated carbon.

Isotherms	Parameters	Values
Langmuir	q_m (mg/g)	149.25
	K_L (L/mg)	8.13×10^{-2}
	R^2	0.934
Freundich	K_F (L/mg)	19.36
	$1/n$	0.47
	R^2	0.882
Temkin	A (L/g)	1.27
	b (J/mol)	97.15
	R^2	0.930

Table 7
Parameters of the kinetic models for RBBR adsorption onto peanut hull-based activated carbon.

Models	Parameters	Values
Pseudo-first-order model	K_1 (min^{-1})	5.52×10^{-2}
	$Q_{e,cal}$ (mg/g)	8.13×10^{-2}
	R^2	0.60
Pseudo-second-order model	K_2 (g/(mg min))	5.52×10^{-4}
	$Q_{e,cal}$ (mg/g)	125
	R^2	0.99

3.3.2. Adsorption kinetics

Numerous kinetic models have been proposed to elucidate the mechanism by which pollutants may be adsorbed. The mechanism of adsorption depends on the physical and/or chemical characteristics of the adsorbent as well as on the mass transport process. To investigate the mechanism of RBBR adsorption on the prepared activated carbon, pseudo-first-order and pseudo-second-order models were considered as follows respectively:

$$\ln(Q_e - Q_t) = \ln Q_e - K_1 t \tag{10}$$

$$\frac{t}{Q_t} = \frac{1}{K_2 Q_e^2} + \frac{t}{Q_e} \tag{11}$$

where Q_e and Q_t (mg/g) are the amount of RBBR adsorbed at equilibrium and at time t (min), respectively. K_1 (min^{-1}) and K_2 (g/(mg min)) are the rate constant of pseudo-first and second-order adsorption rate constants.

The experimental data of RBBR adsorption on the activated carbon indifferent time intervals were examined to fit pseudo-first-order and pseudo-second-order models using the plots of $\ln(Q_e - Q_t)$ against t and t/q_t versus t, respectively. The corresponding results are listed in Table 7. The correlation coefficients, R^2 (Table 7) showed that the pseudo-second-order model, an indication of a chemisorption mechanism could better fitted the experimental data ($R^2 = 0.99$) than the pseudo-first-order model ($R^2 = 0.60$). This revealed that the intraparticle diffusion was involved in the adsorption of RBBR by prepared activated carbon.

4. Conclusions

Response surface methodology was successfully used to investigate the effects of concentration of phosphoric acid, microwave power and radiation time on the adsorption property (expressed in terms of the iodine number) and yield of the prepared activated carbon. The optimum preparation conditions were identified to be a phosphoric acid concentration of 33.04 vol.%, microwave power of 500.70 W and radiation time of 9.8 min, which resulting in 813.11 mg/g of iodine number and 42.12% of carbon yield. The prepared activated carbons exhibited high surface area and well-developed porosity. The BET surface area and total pore volume of optimum samples were 952.6 m^2/g and 0.8807 cm^3/g, respectively.

The activated carbon prepared in the present study was applied to RBBR adsorption. The equilibrium data were best described by the Langmuir isotherm model, indicating that the adsorption of RBBR onto the prepared activated carbon was monolayer and heterogeneous surface adsorption, with adsorption capacity for RBBR of 149.25 mg/g. Peanut hull-based activated carbon was shown to be a promising adsorbent for removal of organic pollutants from aqueous solutions.

Acknowledgements

This work was financially supported by the project of National Natural Science Foundation of China (No. 51078128), International Science & Technology Cooperation Program of China (No.

2011DFA90740), the Hunan Provincial Natural Science Foundation of China (No. 10JJ7005).

References

Abnisa, F., Daud, W.M.A., Sahu, J.N., 2011. Optimization and characterization studies on bio-oil production from palm shell by pyrolysis using response surface methodology. Biomass Bioenergy 35, 3604–3616.

Aguilar, C., García, R., Soto-Garrido, G., Arriagada, R., 2003. Catalytic wet air oxidation of aqueous ammonia with activated carbon. Appl. Catal. B 46, 229–237.

Arami-Niya, A., Daud, W.M.A.W., Mjalli, F.S., Abnisa, F., Shafeeyan, M.S. Production of microporous palm shell based activated carbon for methane adsorption: modeling and optimization using response surface methodology. Chem. Eng. Res. Des., in press.

Azargohar, R., Dalai, A.K., 2005. Production of activated carbon from Luscar char: experimental and modeling studies. Microporous Mesoporous Mater. 85, 219–225.

Basta, A.H., Fierro, V., El-Saied, H., Celzard, A., 2009. 2-Steps KOH activation of rice straw: an efficient method for preparing high-performance activated carbons. Bioresour. Technol. 100, 3941–3947.

Crini, G., 2006. Non-conventional low-cost adsorbents for dye removal: a review. Bioresour. Technol. 97, 1061–1085.

Deng, H., Li, G.X., Yang, H.B., Tang, J.P., Tang, J.Y., 2010. Preparation of activated carbons from cotton stalk by microwave assisted KOH and K_2CO_3 activation. Chem. Eng. J. 163, 373–381.

Deng, H., Yang, L., Tao, G.H., Dai, J.L., 2009. Preparation and characterization of activated carbon from cotton stalk by microwave assisted chemical activation—application in methylene blue adsorption from aqueous solution. J. Hazard. Mater. 166, 1514–1521.

Duan, X.H., Srinivasakannan, C., Peng, J.H., Zhang, L.B., Zhang, Z.Y., 2010. Preparation of activated carbon from Jatropha hull with microwave heating: optimization using response surface methodology. Fuel Process. Technol. 92, 394–400.

Duan, X.H., Srinivasakannan, C., Peng, J.H., Zhang, L.B., Zhang, Z.Y., 2011. Comparison of activated carbon prepared from Jatropha hull by conventional heating and microwave heating. Biomass Bioenergy 35, 3920–3926.

Foo, K.Y., Hameed, B.H., 2011a. Preparation and characterization of activated carbon from pistachio nut shells via microwave-induced chemical activation. Biomass Bioenergy 35, 3257–3326.

Foo, K.Y., Hameed, B.H., 2012. Preparation characterization and evaluation of adsorptive properties of orange peel based activated carbon via microwave induced K_2CO_3 activation. Bioresour. Technol. 104, 679–686.

Foo, K.Y., Hameed, B.H., 2011b. Utilization of rice husks as a feedstock for preparation of activated carbon by microwave induced KOH and K_2CO_3 activation. Bioresour. Technol. 102, 9814–9817.

Freundlich, H.M.F., 1906. Over the adsorption in solution. J. Phys. Chem. 57, 385–470.

Girgis, B.S., Yunis, S.S., Soliman, A.M., 2002. Characteristics of activated carbon from peanut hulls in relation to conditions of preparation. Mater. Lett. 57, 164–172.

Guo, J., Luo, Y., Lua, A.C., Chi, R.A., Bao, X.T., Xiang, S.X., 2007. Adsorption of hydrogen sulphide (H_2S) by activated carbons derived from oil-palm shell. Carbon 45, 330–336.

Hamdaoui, O., 2006. Batch study of liquid-phase adsorption of methylene blue using cedar sawdust and crushed brick. J. Hazard. Mater. 35, 267–273.

Hall, K.R., Eagleton, L.C., Acrivos, A., Vermeulen, T., 1966. Pore- and solid-diffusion kinetics in fixed-bed adsorption under constant-pattern conditions. J. Ind. Eng. Chem. Fundam. 5, 212–223.

Karacan, F., Ozden, U., Karacan, S., 2007. Optimization of manufacturing conditions for activated carbon from Turkish lignite by chemical activation using response surface methodology. Appl. Therm. Eng. 27, 1212–1218.

Li, C.G., Dong, L.Y., Ji, Y.Y., Zhu, Y.F., Fang, S.S., 2010. Study on extraction of cellulose and removal of hemicelluloses and lignin from peanut hull. Chin. Agric. Sci. Bull. 26, 350–354.

Li, W., Zhang, L.B., Peng, J.H., Li, N., Zhu, X.Y., 2008. Preparation of high surface area activated carbons from tobacco stems with K_2CO_3 activation using microwave radiation. Ind. Crops Prod. 27, 341–347.

Liu, Q.S., Zhang, T., Wang, P., Guo, L., 2010. Preparation and characterization of activated carbon from bamboo by microwave-induced phosphoric acid activation. Ind. Crops Prod. 31, 233–238.

Lua, A.C., Guo, J., 2000. Activated carbon prepared from oil palm stone by one-step CO_2 activation for gaseous pollutant removal. Carbon 38, 1089–1097.

Lua, A.C., Yang, T., 2004. Effect of activation temperature on the textural and chemical properties of potassium hydroxide activated carbon prepared from pistachio-nut shell. J. Colloid Interface Sci. 274, 594–601.

Mahalik, K., Sahu, J.N., Patwardhan, A.V., Meikap, B.C., 2010. Statistical modelling and optimization of hydrolysis of urea to generate ammonia for flue gas conditioning. J. Hazard. Mater. 182, 603–610.

Molina-Sabio, M., Rodriguez-Reinoso, F., 2004. Role of chemical activation in the development of carbon porosity. Colloids Surf. A 241, 15–25.

Mudoga, H.L., Yucel, H., Kincal, N., 2008. Decolorization of sugar syrups using commercial and sugar beet pulp based activated carbons. Bioresour. Technol. 99, 3528–3533.

Sahu, J.N., Acharya, J., Meikap, B.C., 2010. Optimization of production conditions for activated carbons from Tamarind wood by zinc chloride using response surface methodology. Bioresour. Technol. 101, 1974–1982.

Weber, T.W., Chakkravorti, R.K., 1974. Pore and solid diffusion models for fixed bed adsorbers. AIChE J. 20, 228–238.

Yagmur, E., Ozmak, M., Aktas, Z., 2008. A novel method for production of activated carbon from waste tea by chemical activation with microwave energy. Fuel 87, 3278–3285.

Yuen, F.K., Hameed, B.H., 2009. Recent developments in the preparation and regeneration of activated carbons by microwaves. Adv. Colloid Interface Sci. 149, 19–27.

Zuo, S.L., Yang, J.X., Liu, J.L., Cai, X., 2009. Significance of the carbonization of volatile pyrolytic products on the properties of activated carbons from phosphoric acid activation of lignocellulosic material. Fuel Process. Technol. 90, 994–1001.